

Mice lacking glial fibrillary acidic protein display astrocytes devoid of intermediate filaments but develop and reproduce normally

Milos Pekny¹, Per Levéen, Marcela Pekna, Camilla Eliasson, Claes-Henric Berthold², Bengt Westermark³ and Christer Betsholtz

Department of Medical Biochemistry, University of Göteborg, Medicinaregatan 9, S-413 90 Göteborg, ²Department of Anatomy and Cell Biology, University of Göteborg and ³Department of Pathology, University of Uppsala, Sweden

¹Corresponding author

Communicated by B.Vennström

Glial fibrillary acidic protein (GFAP) is the main component of the intermediate filaments in cells of astroglial lineage, including astrocytes in the CNS, non-myelin forming Schwann cells and enteric glia. To address the function of GFAP *in vivo*, we have disrupted the GFAP gene in mice via targeted mutation in embryonic stem cells. Mice lacking GFAP developed normally, reached adulthood and reproduced. We did not find any abnormalities in the histological architecture of the CNS, in their behavior, motility, memory, blood–brain barrier function, myenteric plexi histology or intestinal peristaltic movement. Comparisons between GFAP and S-100 immunohistochemical staining patterns in the hippocampus of wild-type and mutant mice suggested a normal abundance of astrocytes in GFAP-negative mice, however, in contrast to wild-types, GFAP-negative astrocytes of the hippocampus and in the white matter of the spinal cord were completely lacking intermediate filaments. This shows that the loss of GFAP intermediate filaments is not compensated for by the up-regulation of other intermediate filament proteins, such as vimentin. The GFAP-negative mice displayed post-traumatic reactive gliosis, which suggests that GFAP up-regulation, a hallmark of reactive gliosis, is not an obligatory requirement for this process.

Key words: blood–brain barrier/gene targeting/glial fibrillary acidic protein/intermediate filaments/reactive gliosis

Introduction

Intermediate filaments (10 nm in diameter) are, together with actin filaments (6 nm) and microtubules (23 nm), components of the cytoskeleton. Intermediate filament proteins constitute a large family of structurally related proteins that show remarkable cell type specificity in their expression (reviewed in Fuchs and Weber, 1994). Data about the *in vivo* functions of several of the intermediate filament proteins have emerged recently. Thus keratins expressed in the epidermis have been found to provide mechanical strength to the skin, as shown by experiments where dominant-negative mutant keratin genes were

expressed in transgenic mice (Vassar, *et al.*, 1991) and by the identification of mutations in keratin genes in individuals with inherited skin disorders affecting the epidermis (Coulombe *et al.*, 1991; Cheng *et al.*, 1992; Chipev *et al.*, 1992; Epstein, 1992; Lane *et al.*, 1992; Rothnagel *et al.*, 1992; Chan *et al.*, 1994; Rugg *et al.*, 1994). Keratins may also perform vital functions during embryogenesis, as suggested by experiments on *Xenopus* embryos, where injected antisense oligonucleotides were found to inhibit gastrulation (Torpey *et al.*, 1992). Disruption of the keratin 8 gene, which is expressed early in mouse development, resulted in embryonic lethality in a proportion of mutant homozygotes (Baribault *et al.*, 1993).

In the central nervous system, neurons co-express three intermediate filament proteins (neurofilaments L, M and H). A spontaneous null mutation in the NF-L gene found in a quiver mutant of Japanese quail leads to a reduction in axonal caliber and generalized quivering (Ohara *et al.*, 1993). Recently, a defect in neurofilaments was suggested to be associated with amyotrophic lateral sclerosis (Côté *et al.*, 1993; Fuchs *et al.*, 1994).

The intermediate filaments of astroglial cells are formed of glial fibrillary acidic protein (GFAP) and vimentin; vimentin filaments are found at early developmental stages, whereas GFAP filaments are present in differentiated and mature brain astrocytes (Chiu *et al.*, 1981). Since GFAP is specifically expressed in astroglial cells, it has become a marker for intracranial and intraspinal tumors arising from these cells (reviewed in Goebel *et al.*, 1987). Apart from being the main component of the intermediate filaments of the cytoskeleton in brain and spinal cord astrocytes, GFAP intermediate filaments are also present in non-myelin forming Schwann cells (Jessen *et al.*, 1990) and enteric glia cells (Jessen and Mirsky, 1983) in the peripheral nervous system.

The function of GFAP intermediate filaments in astrocytes remains obscure. Astrocytes have classically been considered important in providing nutritional and structural support for neurons and for formation of the blood–brain barrier (reviewed in Bignami, 1991). Recently it was suggested that astrocytes also affect functional properties of neurons (Parpura *et al.*, 1994). It is conceivable that some astrocyte functions are dependent on intermediate filaments. For example, a transfected GFAP antisense construct inhibited the protrusion of glial processes *in vitro* (Weinstein *et al.*, 1991). Since during development neurons are believed to migrate to their final positions guided by glial processes, GFAP has been thought of as an important player in the morphogenesis of the central nervous system. GFAP expression *in vivo* is increased in situations connected with astrogliosis, such as brain injury (Goebel *et al.*, 1987), spongiform encephalopathies (Prusiner, 1993) or neuroAIDS (Weis *et al.*, 1993; Toggas *et al.*, 1994). Consequently, it has been suggested that GFAP may play

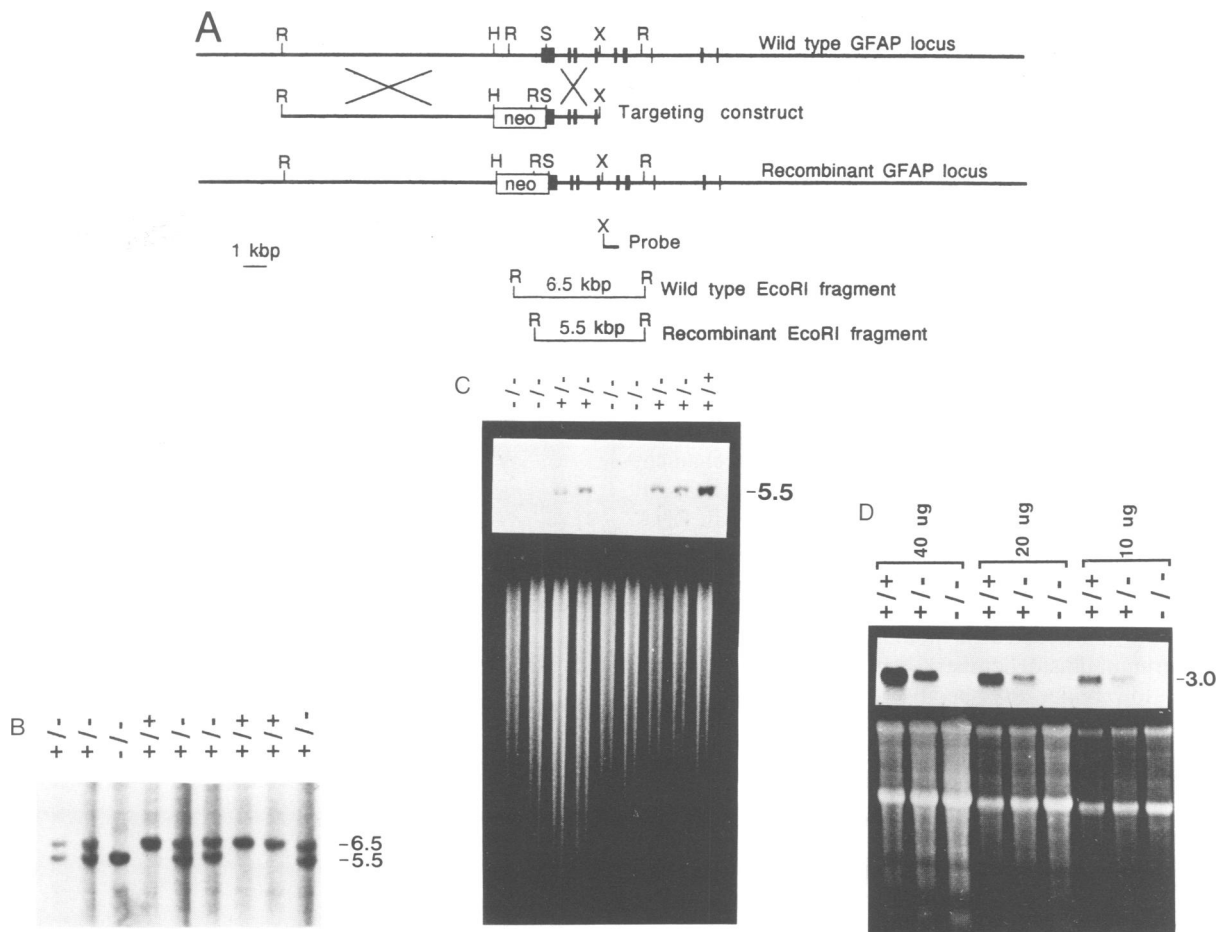


Fig. 1. (A) Targeting strategy for the GFAP locus. R, *EcoRI*; H, *HindIII*; S, *SacI*; X, *XbaI*; the bars indicate exons. (B) Southern blot analysis of tail DNA from the offspring of GFAP^{+/-} parents using the probe indicated in (A). (C) Southern blot analysis of tail DNA from the offspring of GFAP^{+/-} parents using an oligonucleotide probe specific for that part of the GFAP first exon which was deleted in the targeting construct. The figure shows an autoradiogram (top, inset) in comparison with an ethidium bromide stained gel. (D) Northern blot analysis of the total brain RNA from 7-month-old GFAP^{+/+}, GFAP^{+/-} and GFAP^{-/-} mice, using a full-length mouse GFAP cDNA (Lewis *et al.*, 1984) as a probe. An autoradiogram (top, inset) is shown in comparison with an ethidium bromide stained gel. Three different concentrations of RNA were loaded. The size (~3 kb) of the GFAP mRNA is indicated.

a role in the pathogenesis of these disorders. In order to study physiological and putative pathophysiological functions of GFAP *in vivo*, we disrupted the GFAP gene in mice using targeted mutations in embryonic stem cells. The mice deficient for GFAP exhibit normal pre- and post-natal development, reach adulthood, reproduce normally and lack signs of psychomotor abnormalities.

Results

Derivation of GFAP mutant mice

Several overlapping mouse GFAP genomic DNA clones were isolated from a 129SV library and were used to design a targeting construct in which a 5' part of the first exon, encoding the first 71 amino acid residues of the GFAP protein, was deleted, together with 2004 bp of 5' flanking sequence (Figure 1A). This deletion encompasses a region demonstrated to include positive transcriptional regulatory elements that are crucial for GFAP gene expression in both mouse (Miura *et al.*, 1990; Sarid, 1991; Sarkar and Cowan, 1991) and human (Besnard *et al.*, 1991; Masood *et al.*, 1993). The targeting construct was transfected into E14 embryonic stem (ES) cells and

successful targeting to the GFAP locus was identified by Southern blot analyses using a GFAP genomic segment (flanking the targeting construct at the 3' end) as a probe. Three targeted clones were identified among 90 stably transfected, G418-resistant ES cell clones. These three clones were injected into C57BL/6J blastocysts, which were subsequently transferred to foster mothers and allowed to develop to term. Male germline chimeras were derived from two of these ES cell clones and were used to produce heterozygous and subsequently homozygous mutant offspring (Figure 1B) in a mixed 129SV/C57BL/6J genetic background.

Absence of GFAP mRNA and protein in GFAP mutant mice

Mutant offspring were born from heterozygous crosses in the expected ratio (25%), indicating no increased pre-natal lethality in homozygous mutants in comparison with heterozygous and wild-type littermates (Table I). Three lines of evidence suggest that the homozygous mutant mice were entirely devoid of GFAP protein. First, the presence of the expected deletion in the targeted GFAP locus was verified by Southern blot analysis using an

Table I. Genotype of the offspring of parents heterozygous for the GFAP mutant allele (the table does not include other types of crosses also used to generate GFAP-negative offspring)

ES cell clone	Genotype		
	+/+	+/-	-/-
B13	26	42	22
A10	9	17	11
Total	35	59	33

oligonucleotide probe corresponding to the deleted part of the first exon; this probe hybridized to wild-type DNA, with lesser intensity to heterozygous DNA and failed to hybridize to mutant DNA (Figure 1C). This proves that the targeting construct integrated by a replacement mechanism and that the expected deletion was present in the GFAP locus. Second, Northern blot analysis of total brain RNA using a mouse GFAP cDNA probe showed that heterozygous animals had their GFAP mRNA expression reduced by ~50% compared with wild-type animals and no specific signal could be detected in mutant animals (Figure 1D). Finally, immunohistochemistry using anti-GFAP antibodies failed to produce any specific astrocyte staining in the homozygous mutants (Figures 3, 5 and 7).

Normal development of GFAP mutant mice

Mutant, heterozygous and wild-type offspring derived from heterozygous crosses were raised together in order to ease identification of any abnormal development and/or behavior. Neither anatomical/histological differences nor differences in growth and reproductive capacity have been noted between these three genetic groups of animals. Tests focusing on motility, learning and memory (see Materials and methods) did not reveal any consistent differences between the GFAP-negative mice and their heterozygous or wild-type littermates (data not shown).

Brain architecture, histology and GFAP and S-100 expression

Brains from wild-type and mutant animals were serially sectioned and processed for histology and immunohistochemistry using anti-GFAP and anti-S100 antibodies. No significant differences in brain histological architecture were noted (Figure 2A–G). Since the number of GFAP-positive cells in the uninjured adult mouse brain is relatively low, an important question is whether the pool of normally GFAP-positive cells is missing in the mutant brains or whether these cells are present, albeit negative with regard to GFAP. We addressed this question by comparing the expression of GFAP and S-100 protein in wild-type and mutant brains. Although S-100 is expressed by cells of astroglial origin as well as cells of the oligodendrocytic lineage, there are regions of the brain, such as the hippocampus and the immediate surroundings of blood capillaries, where the GFAP and S-100 patterns essentially overlap, indicating that most S-100-positive cells in these regions are also GFAP-positive. We counted GFAP- and S-100-positive cells in the entire hippocampus region of several brain sections to confirm that the numbers were similar (Table II). Whereas GFAP staining was entirely absent in GFAP mutant brains (Figure 3 and data not shown), the numbers of S-100-positive cells in the

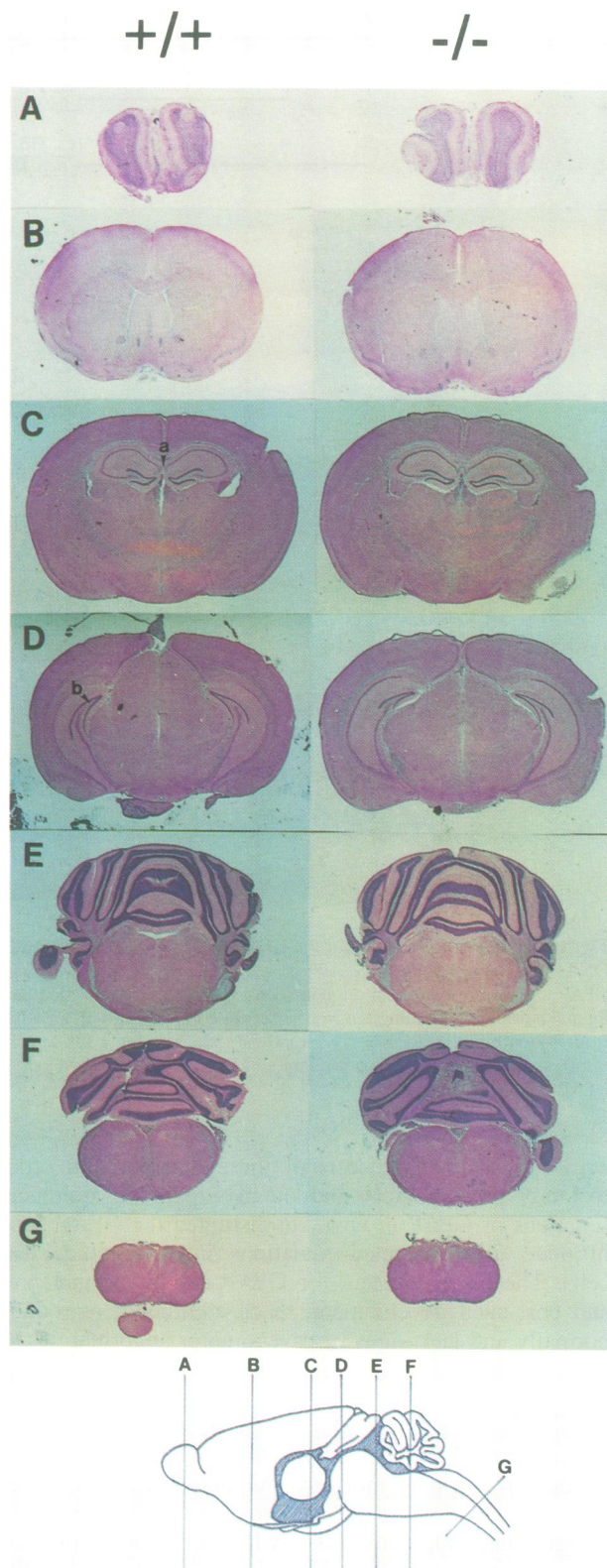


Fig. 2. Histological architecture of control (+/+) and GFAP-negative (-/-) brains from 7-month-old animals. The levels of the transverse sections are illustrated (A–G). Two areas are indicated which are focused on in subsequent analyses in Figure 3B and C (a, arrow in C+/+) and Figure 3A (b, arrow in D+/+). The sections were stained with hematoxylin and erythrosin.

Table II. Number of GFAP- or S-100-positive cells in corresponding hippocampal sections (comparable to Figure 2C) of GFAP+/+ or GFAP-/- mice

	Genotype	
	GFAP+/+	GFAP-/-
GFAP staining	454 ± 13	0
S-100 staining	455 ± 10	438 ± 8

For the comparative quantification of GFAP- and S-100-positive cells, GFAP-positive cells were counted only if a nucleus was present in the section. Data are presented as the mean ± SE.

hippocampus were comparable between wild-type and mutant mice (Table II). Moreover, double immunohistochemistry for GFAP and S-100 demonstrated staining of the same cells in the hippocampus, although GFAP staining localized primarily to cytoplasmic processes and S-100 staining to the nucleus (Figure 3). These data show that the GFAP mutant brains contain normal numbers of astroglial cells, at least in the hippocampus.

Hippocampal astrocytes as well as astrocytes in the spinal cord of GFAP-deficient animals are devoid of intermediate filaments

To elucidate whether intermediate filaments in astrocytes of the mutant mice are present, disorganized or absent, we examined the dentate gyrus of the hippocampus and the lateral funiculus of the spinal cord by electron microscopy. The concave border of the dentate gyrus and the lateral funiculus were screened for sites containing astrocytic cell bodies and their proximal processes. Twenty five such sites were identified in both the control and GFAP-negative mice and the astrocyte cytoplasm was examined directly in the microscope (at 30 000× magnification) for the occurrence of filamentous material. In the control mice all examined sites revealed the presence of parallel bundles of 10 nm intermediate filaments (Figure 4A and C). As expected, the intermediate filaments were more abundant in the fibrous-type astrocytes in the spinal cord, as compared with the protoplasmic-type astrocytes of the dentate gyrus (Privat and Rataboul, 1986). In the GFAP-negative mice all the examined sites showed astrocytes devoid of parallel bundles of 10 nm thick intermediate filaments (Figure 4B and D). No other general ultrastructural differences have been found between the examined areas of the control and mutant mice. Thus, at least in the types of astrocytes examined, the lack of GFAP as a structural material of intermediate filaments does not seem to be compensated for by other intermediate filament proteins and the absence of intermediate filaments in these cells does not lead to any obvious phenotype.

Myenteric plexi in GFAP mutants are GFAP-negative without detectable structural/functional consequences

Myenteric nerve plexi were examined in both GFAP-negative and control mice. As demonstrated in Figure 5, enteric glial cells in the myenteric plexi of the ileum (Figure 5A and B) and colon (Figure 5C and D) of GFAP mutant mice were GFAP-negative, but did not show any difference in S-100 immunostaining in comparison with the control mice (Figure 4E). As an indication of functional

integrity of the GFAP-negative intestinal nerve plexi, we recorded normal peristaltic movements of the intestine immediately post mortem, as well as normal consistency of the feces (data not shown).

Blood-brain barrier function in GFAP mutant mice

It is notable that GFAP-positive cells are abundant in close proximity to blood vessels. This has led to the suggestion that astroglial cells are instrumental in the formation of the blood-brain barrier. To test if this putative function of astroglial cells is dependent on GFAP-containing intermediate filaments, blood-brain barrier function was tested in adult wild-type or GFAP mutant mice by intravenous injection of Evans blue. Successful injection was recorded as an instant blue staining of the skin and was subsequently confirmed by inspection of the viscera and skeletal musculature, which were consistently stained dark blue. Exclusion of this dye from brain parenchyma was evident in both wild-type and mutant animals (Figure 6) and implied the existence of an intact blood-brain barrier in GFAP-negative mice.

Post-traumatic reactive gliosis in GFAP mutant mice

One of the hallmarks of reactive gliosis in response to trauma or neurodegenerative disorders is up-regulated GFAP expression. In response to fine needle injury of the brain of wild-type animals, cells surrounding the needle track displayed a typical pattern of expression of vimentin and GFAP. Generally, three zones of reactive glial cells may be recognized; in the central region, cells staining exclusively for vimentin were found, at an intermediate location, vimentin and GFAP double positive cells were predominant and most distal to the injury, solely GFAP-positive cells were identified (Figure 7). In GFAP mutants, the fine needle injury resulted in scarring which was qualitatively similar to that found in wild-type brains, as judged by light microscopy examination 4 days after injury (Figure 7). During this time, neither wild-type nor mutant animals displayed any post-traumatic symptoms. Mutant brains displayed vimentin up-regulation in cells immediately surrounding the needle track. This was qualitatively similar to the vimentin response in wild-type brains. However, conclusions concerning potential quantitative differences are difficult to draw, since in this kind of experiment the extent of the wound is subject to variation between different animals and different parts of the brain. In addition, it is not possible to quantitatively evaluate the response in astrocytes at a distance from the wound, since GFAP was the only marker for these cells.

Discussion

We report here on the generation of mice which are devoid of GFAP. These mice survive, develop normally and reach adulthood without showing any anatomical, histological or behavioral abnormalities. The absence of GFAP is thus, contrary to predictions (Weinstein *et al.*, 1991), compatible with normal embryonic development and, apparently, the formation of structurally and functionally intact central and peripheral nervous systems.

Comparative S-100 and GFAP immunostaining in mutant and normal mice, together with electron micro-

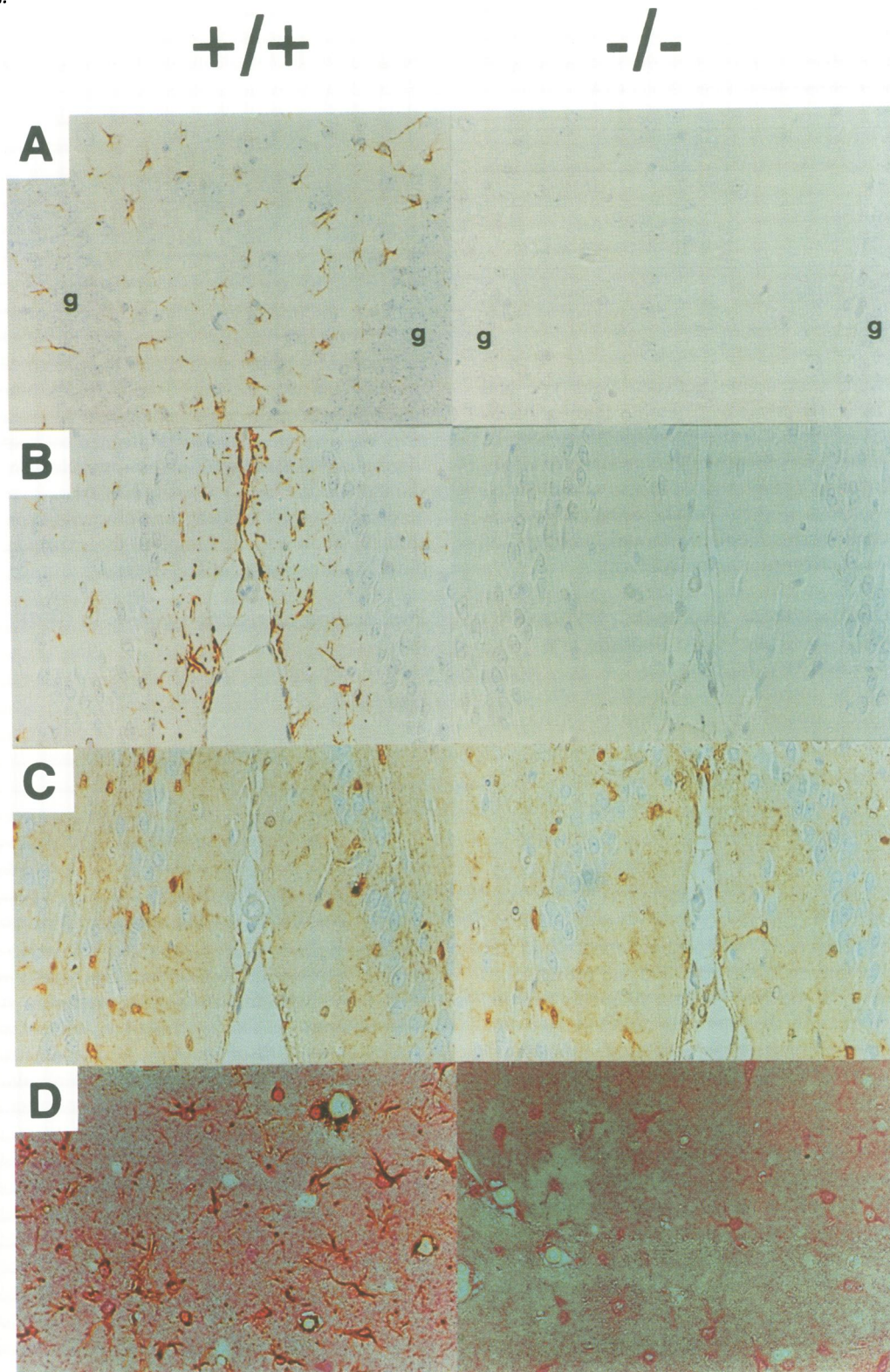


Fig. 3. Sections from the hippocampus (A, see b in Figure 2D; g, granular layer; B and C, see a in Figure 2C) stained with anti-GFAP antibodies (A and B) or anti-S-100 antibodies (C) or both with anti-GFAP (brown staining) and anti-S-100 (red staining) antibodies (D) in control (+/+) and GFAP-negative (-/-) brains from 7-month-old animals. Note that GFAP stains the cytoplasm and the cell processes, whereas the S-100 antibody produces predominantly nuclear and weaker cytoplasmic staining. A, B and C were counterstained with 50× diluted hematoxylin and erythrosin.

scopic examination of selected parts of the central nervous system, suggest that both brain astrocytes and enteric glia are present in the mutants. Thus expression of GFAP appears not to be a prerequisite for the development or tissue distribution of astrocytes. Electron microscopy has

shown the absence of 10 nm thick intermediate filaments in hippocampal astrocytes, as well as in astrocytes in the lateral funiculus of the spinal cord. Thus, at least in these cells, the loss of GFAP does not seem to be compensated for by increased expression of other intermediate filament

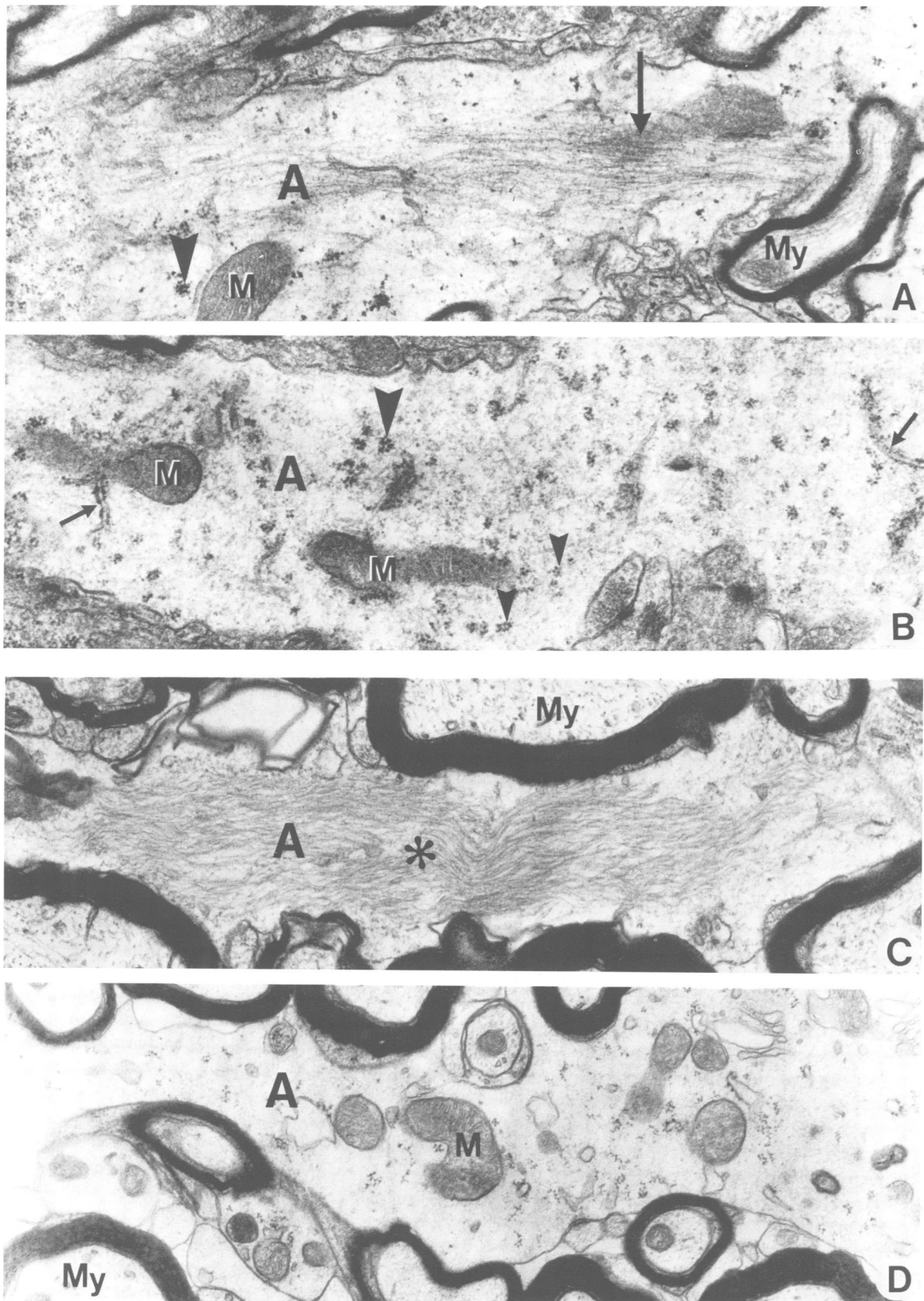


Fig. 4. Electron microscopy of the dentate gyrus of the hippocampus (**A** and **B**) and the lateral funiculus of the upper cervical spinal cord (**C** and **D**). Astrocytes contain bundles of intermediate filaments in the control mice (**A** and **C**). These filaments are absent in the astrocytes of GFAP-deficient mice and their cytoplasm contains only diffuse, low density reticular background material. Intermediate filaments are indicated by a large arrow (**A**) or an asterisk (**C**). A, astrocytic processus; M, mitochondrion; My, myelinated nerve fibers; small arrows show endoplasmic reticulum; large and small arrowheads show rosettes of glycogen particles and polyribosomes respectively. Fixation: glutaraldehyde (**A** and **B**); paraformaldehyde (**C** and **D**). Magnification 29 000 \times .

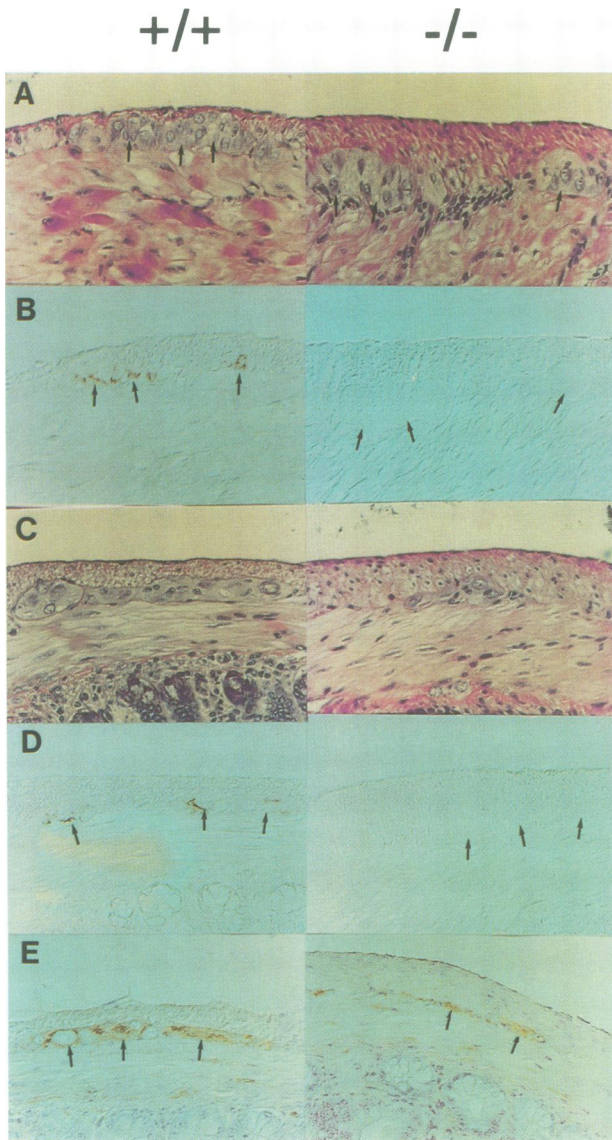


Fig. 5. Myenteric plexus (indicated by arrows) in the ileum (A and B) and colon (C–E) of control (+/+) mice and GFAP-negative (-/-). (A and C) Stained with hematoxylin and erythrosin. (B and D) GFAP immunohistochemistry; (E) S-100 immunohistochemistry; counterstained with 50× diluted hematoxylin and erythrosin.

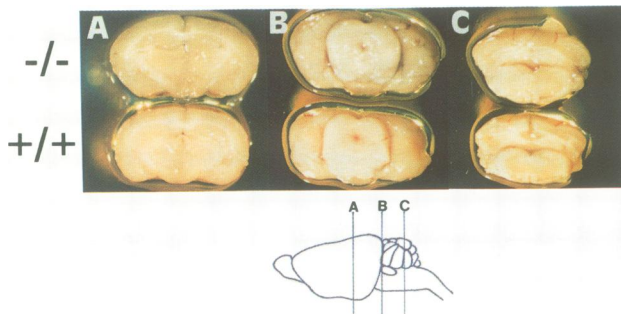


Fig. 6. Blood–brain barrier test. Transverse sections (A–C) through the brain of GFAP-negative (-/-) and control (+/+) mice following i.v. administration of Evans blue. The absence of Evans blue extravasation indicates an intact blood–brain barrier in GFAP-negative mice.

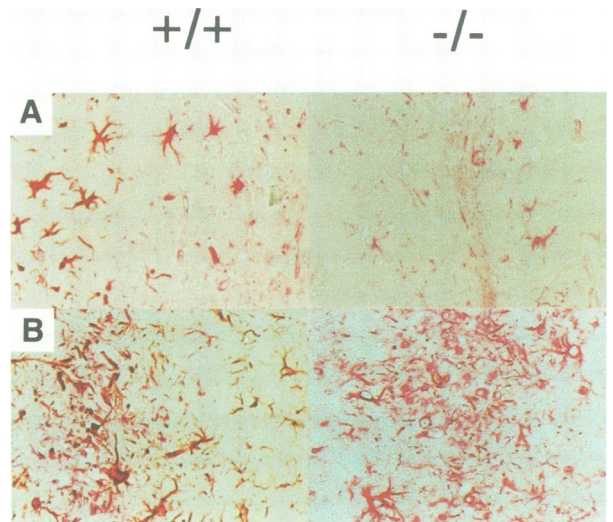


Fig. 7. Reactive gliosis in the cerebral cortex (A) and thalamus (B) of control (+/+) and GFAP-negative (-/-) mice 4 days following a fine needle injury. Immunohistochemical staining with GFAP antibody (brown) and vimentin antibody (red).

proteins. Whether this applies to all types of astrocytes remains to be tested. If the lack of GFAP led to a change in the expression of other intermediate filament proteins, vimentin would be the obvious candidate, since its expression in the astroglial lineage generally precedes that of GFAP. Vimentin and GFAP co-expression has been reported and vimentin–GFAP co-polymer filaments may be formed under certain circumstances (Bjorklund *et al.*, 1984; Calvo *et al.*, 1990; Abnet *et al.*, 1991; Lopez *et al.*, 1992). Using two different vimentin antibodies we have found no indications of changes in the pattern of vimentin expression in GFAP mutants, as determined by immunohistochemical staining of brain sections (data not shown). The overall level of vimentin in the adult mouse brain is, however, very low in the unchallenged state and we were unable to reveal vimentin-positive RNA signals on Northern blots using whole brain RNA from control or mutant mice (data not shown). Although our data do not exclude compensatory expression of other intermediate filament proteins in the GFAP-deficient mice, we show that if such expression occurs, it does not lead to the formation of a 10 nm filamentous network, at least in hippocampal astrocytes and in white matter astrocytes in the spinal cord.

Apparently normal vimentin-negative mice were recently generated (Colucci-Guyon *et al.*, 1994) and the absence of vimentin does not seem to result in compensatory up-regulation of other cytoskeletal intermediate filament proteins in the uninjured brain. The absence of intermediate filaments in vimentin-negative mice was demonstrated in both fibroblasts *in vitro* and lens fibers *in vivo* (Colucci-Guyon *et al.*, 1994). Crosses between GFAP- and vimentin-negative mice are under way to address a potential synergism between these two proteins at specific places or under certain conditions, such as reactive gliosis.

GFAP up-regulation is a hallmark of reactive gliosis triggered by trauma or toxic influences or seen in many neurodegenerative disorders. Here we have studied glial scarring in response to fine needle injury to the brain and

we were unable to disclose any qualitative differences between wild-type and GFAP mutant mice. Although this suggests that the presence of GFAP is not an absolute prerequisite for reactive gliosis in response to trauma, several issues remain to be addressed. Our degree of analysis, for example, could not address quantitative aspects of astrogliosis. Moreover, it does not exclude differences in reactive gliosis in response to other situations, such as toxic stimuli or encephalopathies.

In summary, we have shown here that GFAP intermediate filaments are not required for development of the nervous system. We cannot, however, rule out the possibility that GFAP absence leads either to more subtle changes, which do not result in a recognizable phenotype under laboratory conditions, or to changes which can be seen only in the presence of specific challenges. GFAP absence may also have consequences in conjunction with aging. Experiments are underway to address these issues.

Materials and methods

Derivation of GFAP mutant mice

A phosphoglycerate kinase (PGK) promoter-driven neomycin resistance gene (PGK-neo; kindly provided by Dr J. Heath, Oxford, UK) was used to replace a 2.7 kbp *HindIII*–*SacI* fragment, including the first 233 bp of GFAP exon 1 and 2.0 kbp of 5' flanking sequence, in a targeting construct containing a 9 kbp *EcoRI*–*HindIII* fragment as a 5' homologous segment and a 2.6 kbp *SacI*–*XbaI* fragment as a 3' homologous segment (Figure 1). The homologous segments were all parts of a GFAP genomic clone isolated from a mouse 129SV genomic library in λ FIXII commercially available from Stratagene (La Jolla, CA) using a mouse GFAP cDNA clone as a probe (Lewis *et al.*, 1984) (a kind gift from Dr N. Cowan, NYU Medical Center, New York, NY). The construct was linearized with *NofI* and 50 μ g linearized plasmid were electroporated into the mouse ES cell line E14.1 (kindly provided by Dr R. Kuhn, Cologne, Germany) at passage 18 by electroporation, using a BioRad Gene Pulser set at 260 V, 500 mF. G418-resistant ES cell clones were selected, isolated, frozen and processed for Southern blot analysis as described (Levéen *et al.*, 1994). A 600 bp *XbaI*– λ FIXII-polylinker genomic fragment, flanking the targeting construct at the 3' end, was used to screen for homologous recombination. Recombinant clones, displaying a 5.5 kbp *EcoRI* fragment (in which a novel *EcoRI* site is provided by the PGK-neo cassette) in addition to the wild-type 6.5 kbp *EcoRI* fragment (Figure 1), were thawed, cultured and injected into mouse C57BL6J blastocysts as described (Levéen *et al.*, 1994). Male chimeras were identified by virtue of their fur coat color and high degree chimeras were mated with C57BL6J females. Two of the three isolated recombinant ES clones generated germline chimeras which in both instances were heterozygous and mutant homozygous derived, in agreement with Mendelian allele transmission. All experiments shown have been performed using mice with a hybrid 129/C57BL genetic background. A GFAP exon 1-specific probe was generated using two partially overlapping oligonucleotides, 5'-CTC GGT CCT AGT CGA CAA CTG GGT ACC ATG CCA CGT TTC TCC TTG TCT CGA ATG ACT CCT CCA CTC CCT GCC AGG GTG GA and 5'-CAT CAT CTC TGC ACG CTC GCT CGC CCG TGT CTC CTT GAA GCC AGC ATT GAG CGC CCC GGC CAG GGA GAA GTC CAC CCT GG, which were annealed and radiolabeled using the Klenow fragment of DNA polymerase I and [³²P]dCTP.

Northern blot analyses

Total mouse brain RNA was isolated from wild-type, heterozygous and mutant individuals using the LiCl/urea method (Sambrook *et al.*, 1989) and processed on formaldehyde gels according to standard protocols. The mouse GFAP cDNA described above was labeled using [³²P]dCTP and the Megaprime kit commercially available from Amersham UK.

Histology and immunohistochemistry

Mouse brains were fixed in Bouin's fixative (75 ml saturated picric acid, 5 ml glacial acetic acid, 25 ml 40% formaldehyde), paraffin embedded, sectioned and stained with hematoxylin–erythrosin or processed for immunohistochemistry. For the latter, tissue sections were deparaffinized

and rehydrated. Slides in 0.01 M citric acid, pH 6.0, were heated in a microwave oven twice for 5 min and then incubated at room temperature for 20 min. All the subsequent steps were done at room temperature. Slides were rinsed with phosphate-buffered saline (PBS; 137 mM NaCl, 2.7 mM KCl, 8.1 mM Na₂HPO₄, 1.5 mM KH₂PO₄) and endogenous peroxidase was blocked by incubation in 0.3% H₂O₂ in PBS for 30 min. The slides were then incubated with 0.1% w/v bovine serum albumin (BSA) (Sigma, St Louis, MO) in PBS for 30 min to reduce non-specific background.

Immunohistochemistry for GFAP. Slides were incubated with horseradish peroxidase-conjugated monoclonal antibody against human GFAP (Dako A/S, Glostrup, Denmark). Horseradish peroxidase-conjugated mouse immunoglobulins (Dako A/S, Glostrup, Denmark) were used as the negative control.

Immunohistochemistry for vimentin. Slides were incubated with a rabbit polyclonal antibody against vimentin (Dupouey *et al.*, 1985; a kind gift from E. Colluci-Guyon, Institut Pasteur, Paris, France) in dilution buffer [0.1% w/v BSA, 0.05% v/v Triton X-100 (Sigma, St Louis, MO) in PBS] for 60 min. Normal rabbit serum (Dako A/S, Glostrup, Denmark) was used as the negative control. Sections were then rinsed in PBS and incubated with horseradish peroxidase-conjugated goat antiserum against rabbit immunoglobulins (Dako A/S, Glostrup, Denmark) in dilution buffer for 60 min. In some of the experiments an IgM monoclonal antibody against vimentin (Sigma, St Louis, MO) was used as the primary antibody and normal mouse serum was used as the negative control. In this case, binding of the primary antibody was detected by subsequent incubation of the sections with biotinylated rabbit antibody against mouse IgM (Dako A/S, Glostrup, Denmark) and HRP-conjugated streptavidin (Dako A/S, Glostrup, Denmark).

Immunohistochemistry for S-100. Slides were incubated with a rabbit polyclonal antibody against cow S-100 (Dako A/S, Glostrup, Denmark) in dilution buffer for 30 min. Normal rabbit serum was used as the negative control. Sections were then rinsed in PBS and incubated with horseradish peroxidase-conjugated goat antiserum against rabbit immunoglobulins in dilution buffer for 30 min.

After the last incubation, sections were rinsed in PBS and stained with 3'-diaminobenzidine tetrahydrochloride (DAB; Dako A/S, Glostrup, Denmark) according to the manufacturer's recommendations. The reaction was stopped by rinsing in water and the sections were dehydrated, counterstained with hematoxylin and erythrosin and mounted.

Double immunohistochemistry for GFAP and vimentin. Sections were first incubated with the rabbit polyclonal antibody against vimentin, followed by alkaline phosphatase (AP)-conjugated goat antiserum against rabbit immunoglobulins (Dako A/S, Glostrup, Denmark). Incubation with the antibody against GFAP was then performed as described above.

Double immunohistochemistry for GFAP and S-100. Sections were first stained for S-100 as described above but AP-conjugated goat antiserum against rabbit immunoglobulins was used as the secondary antibody. Sections were then rinsed and incubated with the antibody against GFAP as described above.

After the last incubation, sections were rinsed in PBS and subsequently stained with DAB and Fast Red (Dako A/S, Glostrup, Denmark) according to the manufacturer's recommendations.

Electron microscopy

Two control and two GFAP-negative 3-month-old females were anesthetized with Avertin intraperitoneally. After a vascular rinse with 100 ml Tyrode's solution through the left ventricle, the mice were perfused with 500 ml of either 5% phosphate-buffered paraformaldehyde (one pair) or 5% phosphate-buffered glutaraldehyde (the other pair). The brain and the cervical part of the spinal cord were dissected, post-fixed in the cold overnight and cut into 500 μ m sagittal and transverse sections. The sections were osmicated for 3 h, dehydrated in acetone and embedded in Vestopal 310 (Fluka Chemie, Liechtenstein). The dentate gyrus of the hippocampus and the lateral funiculus of the spinal cord were trimmed out and used for a series of ultrathin (about 100 nm) sections. The sections were processed as previously described (Reynolds, 1963) and examined in a Philips EM 400 electron microscope.

Behavioral studies

For the motility test, mice were placed into a transparent chamber positioned in isolated boxes with one-way windows permitting observation of the animals throughout the experiment. Electric impulses generated by movements within the chamber were recorded over 12 consecutive 5 min intervals.

For the learning and memory test, we used a 30×50 cm bath filled with 25°C milk in which a 5.5×5.5 cm platform was submerged at a fixed position about 1.5 cm under the milk surface level. Mice were placed at the same position in the bath and the time needed to find the platform was recorded repeatedly (learning test) and after 1 h and 1 and 3 days (memory test).

Blood–brain barrier function test

Evans blue [0.2 ml 2% (w/v) solution in PBS] was administered into the circulation via the tail vein. After 4 h, the injected mice were killed, brains were carefully dissected out of the skull and fixed in 4% formalin in PBS for 10 min. Thereafter, the brains were sectioned and photographed.

Brain injury experiment

Anesthetized animals were wounded by the introduction of a 27G fine needle through the skull, the frontal brain cortex and down to the thalamic region. Following this type of injury, neither wild-type nor GFAP mutant animals displayed any recognizable symptoms in the post-traumatic period. Four days after the injury, the animals were killed, brains were carefully dissected out of the skull, fixed in Bouin's fixative and processed for histology and immunohistochemistry.

Acknowledgements

We thank Dr R.Feinstein (The National Veterinary Institute, Uppsala, Sweden) for help with the histological analyses of the mice, Dr B.Söderpalm (Department of Pharmacology, Göteborg, Sweden) for help with motility tests and Drs C.Babinet (Institut Pasteur, Paris, France) and S.Itohara (Institute for Virus Research, Kyoto, Japan) for sharing results prior to publication. Dr R.Kuhn (Cologne, Germany) is acknowledged for E14.1 ES cells, Dr J.Heath (Oxford, UK) for the PGK-neo cassette and Dr E.Colucci-Guyon (Institut Pasteur, Paris, France) for the vimentin antibody. This study was supported by grants from the Swedish Cancer Foundation; part of this work was supported by the Swedish MRC, project 03157.

References

- Abnet,K., Fawcett,J.W. and Dunnett,S.B. (1991) *Brain Res. Dev. Brain Res.*, **59**, 187–196.
- Baribault,H., Price,J., Miyai,K. and Oshima,R.G. (1993) *Genes Dev.*, **7**, 1191–1202.
- Besnard,F., Brenner,M., Nakatani,Y., Chao,R., Purohit,H.J. and Freese,E. (1991) *J. Biol. Chem.*, **266**, 18877–18883.
- Bignami,A. (1991) *Discussions in Neuroscience*. Elsevier Science Publishers, Amsterdam, Vol. VIII, pp. 1–45.
- Bjorklund,H., Eriksdotter,N.M., Dahl,D. and Olson,L. (1984) *Med. Biol.*, **62**, 38–48.
- Calvo,J.L., Carbonell,A.L. and Boya,J. (1990) *Brain Res.*, **532**, 355–357.
- Chan,Y., Anton-Lamprecht,I., Yu,Q.-C., Jäckel,A., Zabel,B., Ernsts,J.P. and Fuchs,E. (1994) *Genes Dev.*, **8**, 2574–2587.
- Cheng,J., Syder,A.J., Yu,Q.C., Letai,A., Paller,A.S. and Fuchs,E. (1992) *Cell*, **70**, 811–819.
- Chipev,C.C., Korge,B.P., Markova,N., Bale,S.J., DiGiovanna,J.J., Compton,J.G. and Steinert,P.M. (1992) *Cell*, **70**, 821–828.
- Chiu,F.C., Norton,W.T. and Fields,K.L. (1981) *J. Neurochem.*, **37**, 147–155.
- Colucci-Guyon,E., Portier,M.-M., Dunia,I., Paulin,D., Pournin,S. and Babinet,C. (1994) *Cell*, **79**, 679–694.
- Coulombe,P.A., Hutton,M.E., Letai,A., Hebert,A., Paller,A.S. and Fuchs,E. (1991) *Cell*, **66**, 1301–1311.
- Côté,F., Collard,J.F. and Julien,J.P. (1993) *Cell*, **73**, 35–46.
- Dupouey,P., Benjelloun,S. and Gomes,D. (1985) *Dev. Neurosci.*, **7**, 81–93.
- Epstein,E.J. (1992) *Science*, **256**, 799–804.
- Fuchs,E. and Weber,K. (1994) *Annu. Rev. Biochem.*, **63**, 345–382.
- Fuchs,E., Chan,Y., Paller,A.S. and Yu,Q.-C. (1994) *Trends Cell Biol.*, **4**, 321–326.
- Goebel,H.H., Schlie,M. and Eng,L.F. (1987) *Acta Histochem.*, **34** (suppl.), 81–93.
- Jessen,K.R. and Mirsky,R. (1983) *J. Neurosci.*, **3**, 2206–2218.
- Jessen,K.R., Morgan,L., Stewart,H.J. and Mirsky,R. (1990) *Development*, **109**, 91–103.
- Lane,E.B., Rugg,E.L., Navsaria,H., Leigh,I.M., Heagerty,A.H., Ishida,Y.A. and Eady,R.A. (1992) *Nature*, **356**, 244–246.

- Levéen,P., Pekny,M., Gebre-Medhin,S., Swolin,B., Larsson,E. and Betsholtz,C. (1994) *Genes Dev.*, **8**, 1875–1887.
- Lewis,S.A., Balcarek,J.M., Krek,V., Shelanski,M. and Cowan,N.J. (1984) *Proc. Natl Acad. Sci. USA*, **81**, 2743–6.
- Lopez,M.F., Calvo,J.L., Boya,J. and Carbonell,A.L. (1992) *J. Pineal Res.*, **12**, 145–148.
- Masood,K., Besnard,F., Su,Y. and Brenner,M. (1993) *J. Neurochem.*, **61**, 160–166.
- Miura,M., Tamura,T. and Mikoshiba,K. (1990) *J. Neurochem.*, **55**, 1180–1188.
- Ohara,O., Gahara,Y., Miyake,T., Teraoka,H. and Kitamura,T. (1993) *J. Cell Biol.*, **121**, 387–395.
- Parpura,V., Basarsky,T.A., Liu,F., Jeftinija,K., Jeftinija,S. and Haydon,P.G. (1994) *Nature*, **369**, 744–747.
- Privat,A. and Rataboul,P. (1986) In Fedoroff,S. and Vernadakis,A. (eds), *Astrocytes. Development, Morphology and Regional Specialization*. Academic Press, Vol. I, pp. 105–129.
- Prusiner,S.B. (1993) *Arch. Neurol.*, **50**, 1129–1153.
- Reynolds,E. (1963) *J. Cell Biol.*, **17**, 207–217.
- Rothnagel,J.A. *et al.* (1992) *Science*, **257**, 1128–1130.
- Rugg,E.L. *et al.* (1994) *Genes Dev.*, **8**, 2563–2573.
- Sambrook,J., Fritsch,E.F. and Maniatis,T. (1989). *Molecular Cloning. A Laboratory Manual*. Cold Spring Harbor Laboratory Press, Cold Spring Harbor, NY.
- Sarid,J. (1991) *J. Neurosci. Res.*, **28**, 217–228.
- Sarkar,S. and Cowan,N.J. (1991) *J. Neurochem.*, **57**, 675–684.
- Toggas,S.M., Masliah,E., Rockenstein,E.M., Rall,G.F., Abraham,C.R. and Mucke,L. (1994) *Nature*, **367**, 188–193.
- Torpey,N., Wylie,C.C. and Heasman,J. (1992) *Nature*, **357**, 413–415.
- Vassar,R., Coulomb,P.A., Degenstein,L., Albers,K. and Fuchs,E. (1991) *Cell*, **64**, 365–380.
- Weinstein,D.E., Shelanski,M.L. and Liem,R.K. (1991) *J. Cell Biol.*, **112**, 1205–1213.
- Weis,S., Haug,H. and Budka,H. (1993) *Neuropathol. Appl. Neurobiol.*, **19**, 329–335.

Received on November 14, 1994; revised on January 25, 1995